Effect of Alloy Additions on Wear Resistance of Nickel Based Hardfacing

Different electrode combinations are tried to see which gives the best wear resistance

BY Y. L. SU AND K. Y. CHEN

ABSTRACT. The purpose of this research is to study the influence of the microstructure and hardness of the nickel based hardfacing alloy on wear resistance of deposit layers when different alloy elements are added. Different deposit layers were obtained by SMAW in which AWS RNiCr bare electrodes were coated by fluxes, to which different measures of ferro-niobium, ferrochromium, and carbon had been added. The result of the experiment showed that when subject to abrasive wear, if the abrasive particles were silicon carbide, the increase of the volume fraction of the hard phase had only a slight effect on improving the wear resistance of the deposit layers. However, if the abrasive particles were quartz, the increase of the volume fraction of the hard phase could improve the wear resistance of the deposit layers. On adhesive wear, the niobium added specimens formed some spherical niobium carbide particles in the matrix of the deposit layer which reduced the friction coefficient of the specimens. The addition of carbon and chromium can enhance macrohardness and wear resistance of the welding deposit significantly. This same addition will also aid wear resistance by forming a continuous phase in the microstructure of the deposit metal. While there was no significant difference between the macrohardnesses of the metals, the form of this precipitate in the deposit metals was actually the most important factor in their wear resistance. In the corrosion test, we found that increased carbon content reduced corrosion resistance to nitric acid. Increased chromium content helped to resist corrosion caused by nitric acid, but adversely affected corrosion resistance to hydrochloric acid.

Y. L. SU is a professor and K. Y. CHEN is a graduate student with the Department of Mechanical Engineering at the National Cheng Kung University, Tainan, Taiwan.

Introduction

Wear of machine components or tools is one of the most common problems faced in industry today. The process of hardfacing reduces the effects of wear. A coating of hardfacing material is applied to the surface of a machine component or tool as a welding deposit. This formed deposit imparts better wear resistance and reduces wear and tear on machine components or tools (Refs. 1–4). Utilizing hardfacing material to coat the surfaces of machine components or tools, such as mineral deposit mining equipment, the parts of stone clusters, extruder screws, pump and fan impellers, machine ways, etc., not only helps them resist abrasive wear and adhesive wear, but also helps to prevent corrosion and high temperature oxidation.

There are many advantages to applying hardfacing to the worn components of a machine, especially when these components are large or expensive. Repairing them by hardfacing can be done immediately and inexpensively, without disassembly or reassembly of the machine, and thus no loss of production. In addition, the deposit layers on the components enable greater external loading of the machine, increasing production efficiency.

KEY WORDS

Nickel Based Alloy
Hardfacing
Abrasive Wear
Adhesive Wear
Niobium Carbide
Chromium Carbide

Some literature (Refs. 5, 6) tries to predict material wear resistance by using mechanical or physical criteria, among these, hardness is a very useful index. However, hardness is not the only factor in determining wear resistance. Most of the materials consist of several different hard phases, the sizes and distributions of which change their wear resistance even when the macrohardness of these materials is the same.

Generally speaking, to obtain better wear resistance, we must try to acquire high hardness, coarse secondary phase precipitate while the microstructure is growing. When subjected to abrasive wear, the wear resistance of the deposit layers is improved by increasing the volume fraction of the carbide phase, the result of an increase in carbun cuntent (Refs. 7, 8). Some research points out that matrix composition, and the interface between hard particle and matrix affect wear much more than does the volume fraction of hard phase in adhesive wear (Refs. 9, 10). This theory contradicts the fact that, as the volume fraction of hard phase increased, the wear resistance improved. Therefore, to improve the metal-to-metal adhesive wear resistance, it is necessary to improve the matrix.

Hardfacing materials were first developed as cast CoCr alloys. Later, to increase the corrosion resistance and high temperature strength, NiCr materials came into the field. The next development was to increase the portion of hard chromium carbide precipitates in the soft, austenitic nickel matrix, which were produced by the addition of 0.5~1% carbon. Finally, by adding boron and silicon (about 4% each), the NiCrBSi materials were formed. There were two effects resulting from the addition of boron and silicon: 1) Increased precipitation of hard phase particles (e.g.,

boron compounds, silicon compounds); and 2) A significant appearance of self-fluxing behavior from the boron silicates formed at 900°C (1652°F). The microstructure consisted of a niobium-rich matrix with precipitation of Ni_3B, Cr_2B, CrB, chromium carbide, and a small amount of $(Cr, M)_7C_3$ carbide (Ref. 11).

In recent developments, several alloy elements were introduced as additives to NiCrBSi to acquire high hardness, coarse secondary phase precipitate, such as the addition of niobium or molybdenum to form niobium carbide and molybdenum boride. But research in this field is limited, and too much emphasis is usually placed on discussing abrasive wear (Ref. 12). Thus, this research was conducted to systematically study the adhesive wear, in addition to the abrasive wear of nickel based hardfacing alloy when combined with several different compositions of additional alloy elements.

Experimental Details

Hardfacing

In this research, deposit layers with different alloy contents were obtained by the following steps:

1) Different covered electrodes were produced by using AWS RNiCr bare electrodes and coating them with fluxes containing different measures of ferro-niobium, ferro-chromium, and carbon. The diameter ratio (D/d) was 6.7/4.

2) Surfacing of the SMAW was done on the steel plates. During the remelting process, the alloying element in the fluxes transited to the deposit layers, thus deposit metals with different alloy contents were obtained.

The surfacing was placed upon AISI 1045 carbon steel plates using manual shielded metal arc welding under direct current with a reverse polarity. The plates were air blasted prior to welding to remove stains and other contaminants from their surfaces. To reduce the internal stresses produced during welding, the carbon steel plates were preheated by a neutral oxygen-acetylene flame at approximately 250°C (482°F) before welding. To assure the dryness of the electrode, it was also baked in the furnace at 250°C for 3 h. During welding, to avoid the effect of dilution, hardfacing was welded in a 2 mm thick layer, and then the surfacing on the second and the third layer were done with the same electrodes, which were about 3 mm thick, and with an interpass temperature of about 250°C. The other welding parameters were as follows: welding current 160–170 A, arc voltage 20–21 V, electrode traveling speed 20 cm/min. Under those conditions, a plate covered by deposit layers was produced.

Metallography, Composition and Hardness

Samples were cut from the steel plate using an abrasive cutting machine and then mounted. Next, they were ground using No. 1200 silicon carbide abrasive paper, and polished with 1 mm and 0.3 mm grain size Al_2O_3 powder, cleaned in an ultrasonic cleaner with acetone, dried, etched and their microstructures were then observed, using both an optical microscope (OM) and a scanning electron microscope (SEM).

Macrohardness of the deposit layers was determined by using the average of five measurements taken from the surface of the deposit layers. To determine hardness variations of the deposit layer, data were measured at 0.2 mm intervals, starting from the base metal and moving toward the deposit layer. SEM-EDAX analysis on small areas was used to confirm whether composition was uniform or not.

Abrasive Wear Test

The abrasive wear test was conducted using an ASTM G65 dry sand/rubber wheel abrasion testing machine. Figure 1 shows a schematic diagram of the ASTM G65 (Ref. 13). There were two kinds of testing abrasives, quartz and silicon carbide. (Quartz was the standard test sand of ASTM G65, and the particle sizes of the silicon carbide were: 20 mesh, 0%; 42 mesh, 92%; 60 mesh, 95%; 150 mesh, 100%). The surface roughness of the wear specimens was controlled under Ra = 0.8 mm. The testing parameters were: load 130 N, sand flow rate 300 g/min, wheel rotation velocity 200 rpm, wheel diameter 228.6 mm, and testing time was 10 min. The total distance of wear was 1436 m. Before and after the test, all the specimens were cleaned using an ultrasonic cleaner, and then weighed on an electron balance. The abrasives were also baked at 150°C (302°F) in the furnace for 1 h before the test.

Wear testing was conducted using an SRV oscillating point-contact wear machine produced by the Optimol Co. (Germany). The coefficient of friction, in addition to the load, stroke and temperature, were recorded in real time by a computerized data acquisition system (DAS) equipped with an analog/digital (A/D) converter. A PC286-AT computer received the data and wrote them immediately to its hard disk. An upper specimen was in contact with the flat side of a lower hardfacing specimen, and oscillated horizontally. The dimensions of the test specimens and a schematic diagram of the experiment setup are shown in Fig. 2. The testing parameters were:

lubrication condition:	dry wear	HD150
upper specimen:	Si_3N_4 ceramic ball	Cr steel ball
load:	15 N	300 N
frequency:	50 Hz	50 Hz
stroke:	0.5 mm	0.5 mm
time:	12 min	24 min

The lubricant used for the test was HD150, produced by the China Petroleum Company. The kinematic viscosity of HD150 is 138.9 and 14.4 cSt at 40°C (104°F) and 100°C (212°)

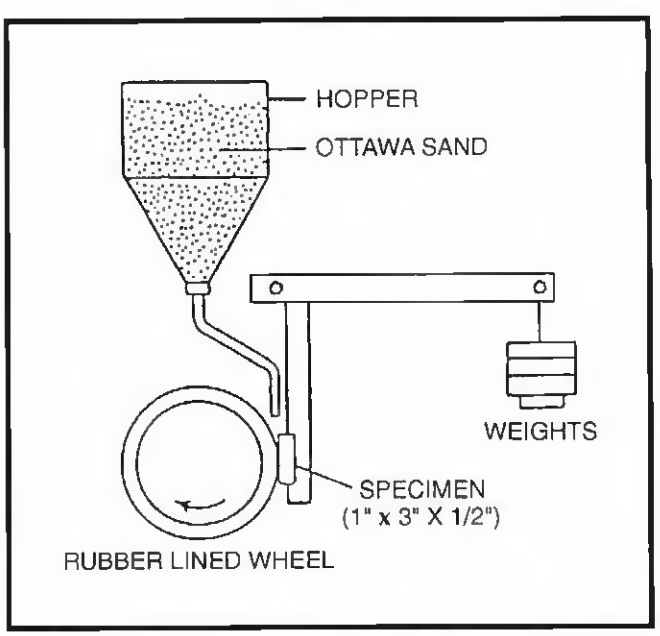

Fig. 1 — Schematic diagram, ASTM G65 dry sand/rubber wheel abrasion testing machine.

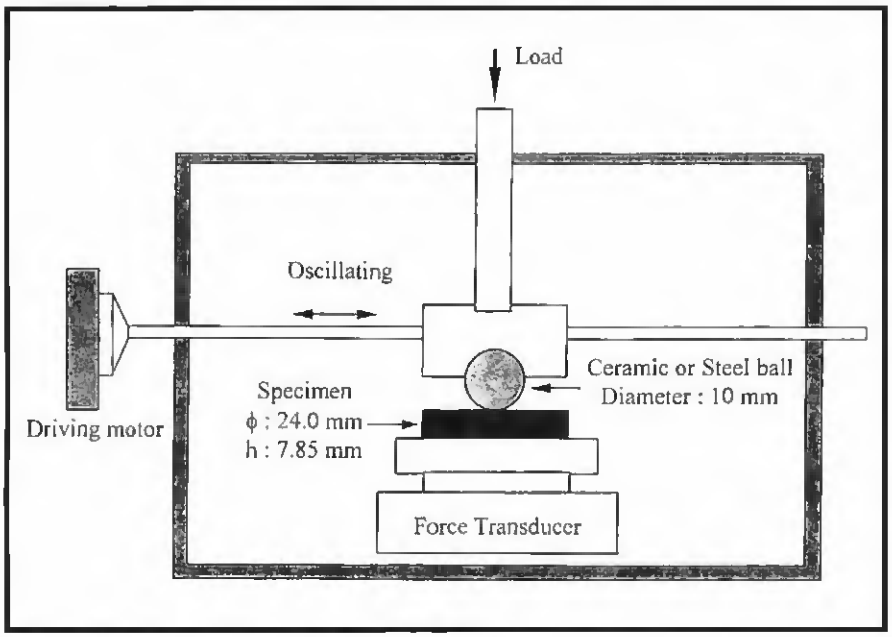

Fig. 2 — Schematic diagram, SRV wear testing machine.

respectively. The surface roughness of the lower specimens was controlled in the range of Ra = 0.075 ~ 0.085 mm. The tests were conducted at room temperature and atmospheric pressure. The relative humidity of the laboratory was about 45–50%. A profilometer was used to measure the dimensions of the wear scar on the specimens. Wear was evaluated by wear scar depth and wear scar width for the lower specimen parts.

Corrosion Test

Different samples for the same plate were exposed to 20% nitric acid solution and 20% hydrochloric acid solution respectively for 100 h at room temperature. They were then removed from the solution, cleaned, dried, and their weight loss determined so the effects of the different alloy elements and their corrosion resistance could be observed.

Results and Discussion

To determine variations in the composition and hardness of the deposit layer, analysis of the nickel and niobium elements was done by SEM-EDAX on a cross section of the sample, moving upward gradually from the interface to the surface. The result is shown in Fig. 3. The nickel and niobium content became steady when the distance was about 3–4 mm from the interface. Furthermore, the hardness of the deposit layer tended to be constant when the upward distance from the interface was 3–4 mm—Fig. 4. Thus, reliable compositions will be obtained when the thickness of the deposit layers is controlled at over 4 mm.

Metallograph, Chemical Composition, and Hardness

In Table 1, the chemical composition and macrohardness values for each of the specimens are listed. These data were measured beginning with the top layer of the deposit layers. Figure 5A was the metallograph of Specimen No. Nb0, which was the commercial Ni-Cr-B-Si alloy AWS ENiCr-A. The microstructures initially showed a solidified coarse hard chromium boride of MB type, embedded in an Ni_3B/Ni-eutectic and/or in a nickel metal matrix hardened by the dissolved chromium and silicon. Figure 5B was the metallograph after the niobium element was added, with spherical particles of the precipitates of niobium carbide uniformly distributed throughout the microstructure. Figure 5C was the metallograph of CNb3 deposit, which shows that both the number of precipitates and the size of the niobium carbide grew much larger. Figure 6 shows the relationship between macrohardness and niobium content. Macrohardness is gradually reduced when the niobium content is increased (from Nb0 to Nb3), possibly attributable to the strong affinity between niobium and carbon. The aforementioned of the two elements could produce precipitates of niobium carbide, which would then cause the carbon content in the matrix to decline, reducing its hardness. By adding niobium and carbon simultaneously, the volume fraction of the hard phase particles increases with only a slight increase in the hardness of the matrix. Similar to the addition of niobium, when the chromium content is increased, the macrohardness of Specimens No. Cr0 to No. Cr3 is reduced. The difference between them is that when chromium is added, the shape of the precipitates

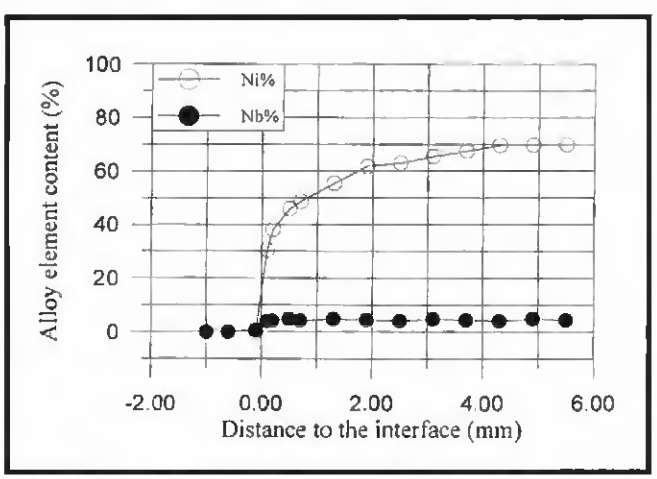

Fig. 3 — The variation of the alloy content of the deposit layers.

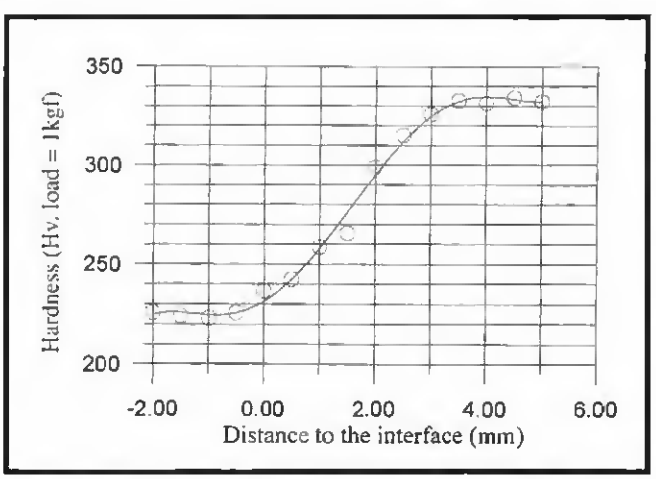

Fig. 4 — The variation in macrohardness of the deposit layers.

Table 1—Chemical Composition and Macrohardness of the Deposit Layers

	C	Si	Mn	Cr	Fe	Mo	Nb	B	Ni	Hv
Nb0	0.23	4.40	0.52	14.43	4.43	0.22	0.02	0.90	Bal.	345
Nb1	0.21	4.07	0.54	14.77	5.33	0.26	1.01	0.84	Bal.	340
Nb2	0.20	3.73	0.52	14.66	5.69	0.29	2.13	0.85	Bal.	336
Nb3	0.20	3.61	0.53	14.25	6.22	0.35	4.37	0.83	Bal.	332
CNb0	0.74	4.69	0.59	14.93	4.54	0.31	0.02	1.04	Bal.	382
CNb1	0.67	4.61	0.63	15.11	4.94	0.32	1.25	0.98	Bal.	410
CNb2	0.56	4.54	0.60	14.86	5.14	0.33	2.09	0.98	Bal.	402
CNb3	0.47	4.11	0.54	14.33	5.88	0.37	3.88	0.93	Bal.	386
Cr0	0.20	4.28	0.50	14.52	4.69	0.22	0.02	1.07	Bal.	366
Cr1	0.20	4.22	0.58	16.62	4.58	0.24	0.02	0.97	Bal.	352
Cr2	0.17	3.97	0.57	18.33	4.74	0.26	0.02	0.86	Bal.	345
Cr3	0.16	3.87	0.56	21.03	4.67	0.29	0.03	0.90	Bal.	340
CCr0	1.22	4.88	0.63	14.92	4.02	0.37	0.03	1.06	Bal.	553
CCr1	1.17	4.76	0.64	16.60	4.22	0.38	0.03	1.10	Bal.	614
CCr2	1.06	4.72	0.65	18.01	4.31	0.39	0.03	1.06	Bal.	649
CCr3	0.91	4.73	0.62	21.05	4.49	0.39	0.03	1.03	Bal.	584

becomes an irregular short rod or small particle—Fig. 7A. When chromium and carbon were added simultaneously, they formed a continuous structure in the microstructure whose carbon content was great and whose hardness was high, so the macrohardness of the deposit layer increased considerably—Fig. 7B. But when the chromium content continued to increase, the continuous structure disappeared, and instead of lenticular chromium carbide precipitates, the carbon elements in the matrix were depleted, thus reducing the macrohardness—Fig. 7C. Figure 8 shows the relationship between macrohardness and chromium content. Figure 8 indicates that the hardness of the materials increased considerably when carbon and chromium were added simultaneously. However, with the increased chromium content, the macrohardness of the materials rose to a maximum value, then dropped down.

The composition of alloys AWS RNiCr-A, RNiCr-B, and RNiCr-C, as shown in Table 2, were quite similar (Ref. 14). But in fact, of the minor variance in carbon and boron elements was the main cause macrohardness increases from about 35 HRC in the A alloys to as high as 60 HRC in the C alloys. This phenomenon resulted from the effects of solution hardening and second phase particle effect on the carbon and boron in the nickel matrix. The nickel based hardfacing alloy could not be hardened by heat treatment, and so was used as the deposit. An iron based alloy can reach the same hardness as the nickel based alloy when heat treated, but the latter still has better wear resistance (Ref. 15).

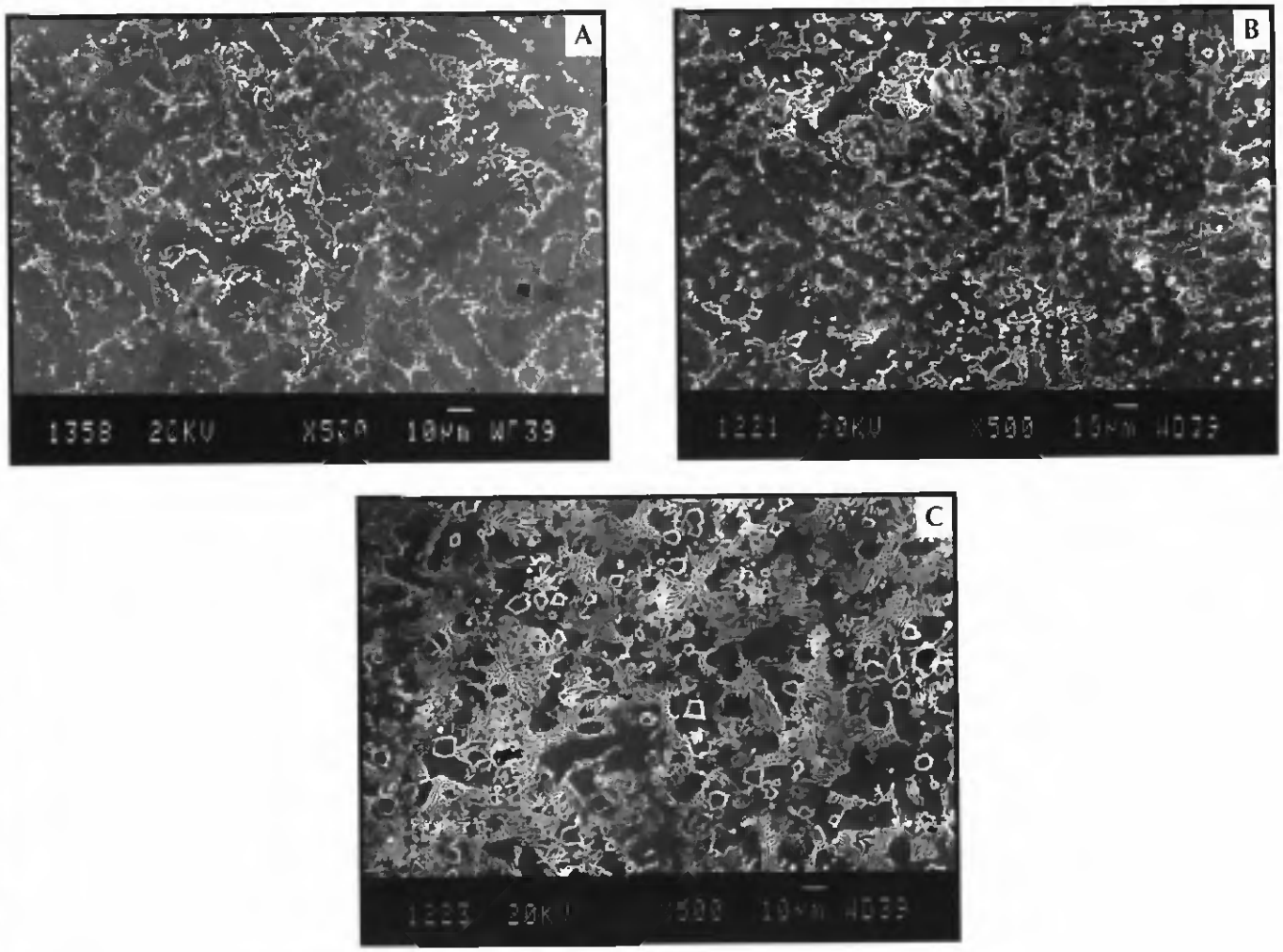

Fig. 5 — The microstructure of the niobium and CNb deposit layers. A — No. Nb0. B — No. Nb3. C — No. CNb3.

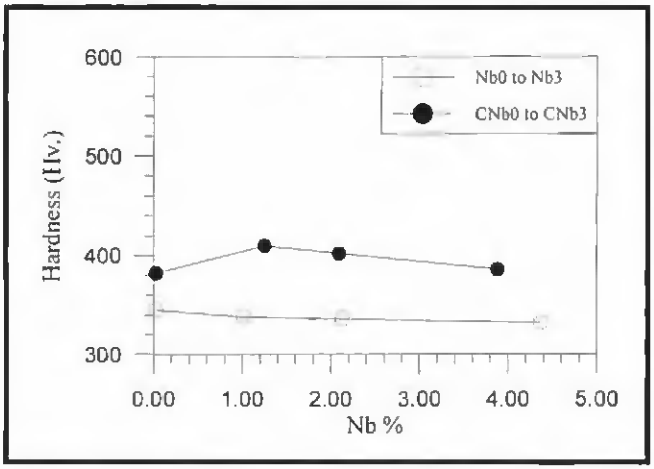

Fig. 6 — The relationship between macrohardness and niobium content.

Abrasive Wear Test

Table 3 depicts the results of the abrasive wear test showing weight loss in deposit layers. Figure 9 shows the deposit layer weight loss results plotted against the hardness as determined by the abrasive wear test. Scattering bands for the two abrasive particles could be observed. When the macrohardness increased, for hard particles such as silicon carbide, the weight loss of the deposit layers varied insignificantly; conversely, for softer particles like quartz, the wear resistance was improved. Hurricks (Ref. 16) pointed out that abrasive wear resistance was related to the hardness ratio between the abrasive and the deposit layers—the lower the hardness, the lower the wear loss. Because of the high hardness of silicon carbide particles (Hv = 2585), all hard phase in the microstructure would be reduced. This effect slightly increased the volume fraction of the hard particles and raised the macrohardness. But for quartz, because its Knoop hardness value is about 840 Hk, wear resistance was increased by increasing the volume fraction of hard phase particles.

Table 4 depicts the results of the adhesive wear test showing wear scar depth in deposit layers. Figure 10 shows the results of the SRV adhesive wear test under dry wear. The upper specimen was Si_3N_4 ball. Generally speaking, the wear loss gradually diminished when microhardness increased, but as far as the addition of different alloy elements was concerned, the phenomena will be different. When only niobium was added to the flux, though the macrohardness of the deposit layers diminished as the niobium content increased, the wear scar depth decreased. In Fig. 11, the relationship between niobium content and wear scar depth is shown. The aforementioned phenomenon relates to the particles of niobium carbide. The

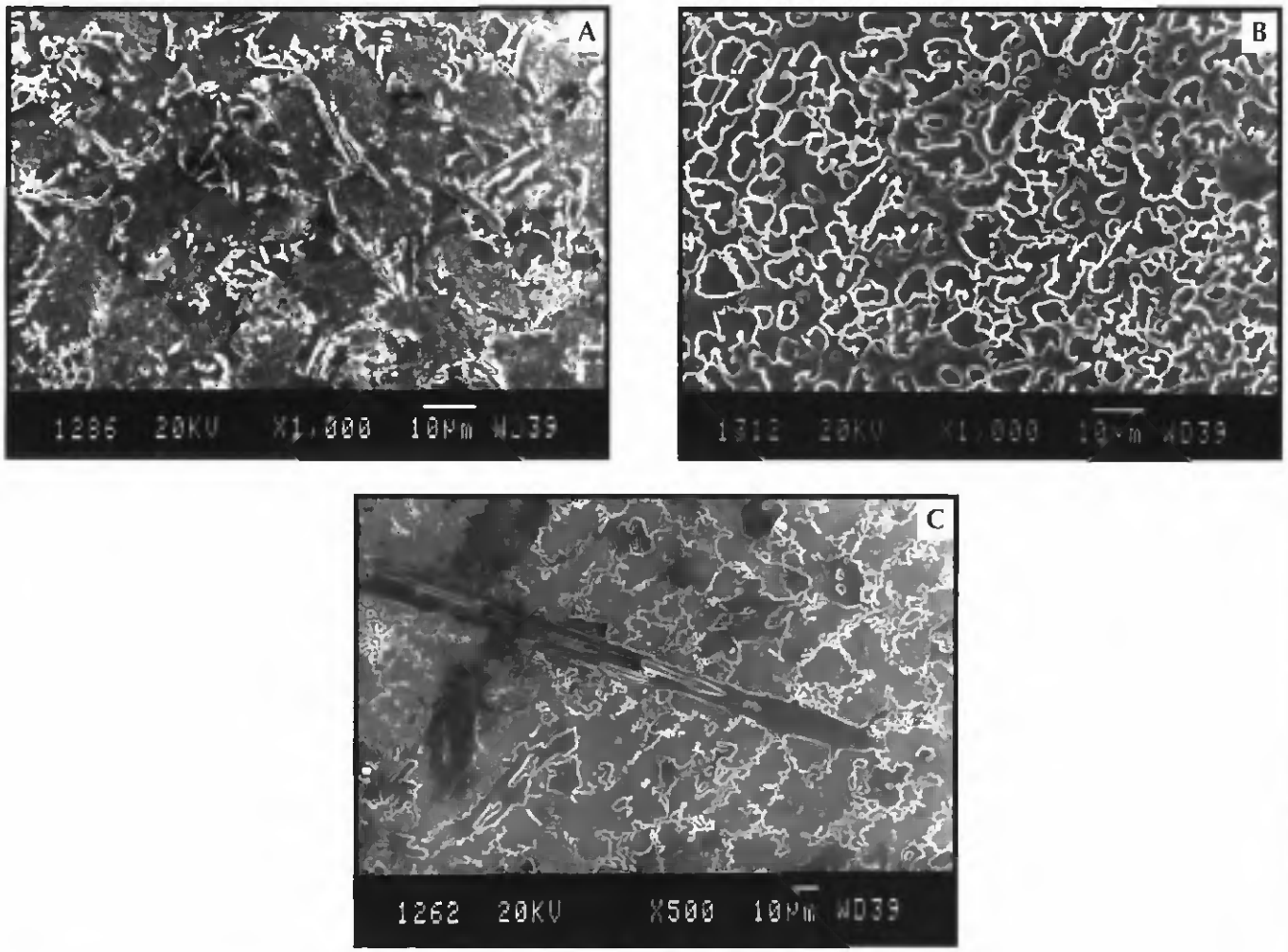

Fig. 7 — The microstructure of the chromium and CCr deposit layers. A — No. Cr3. B — No. CCr2. C — No. CCr3.

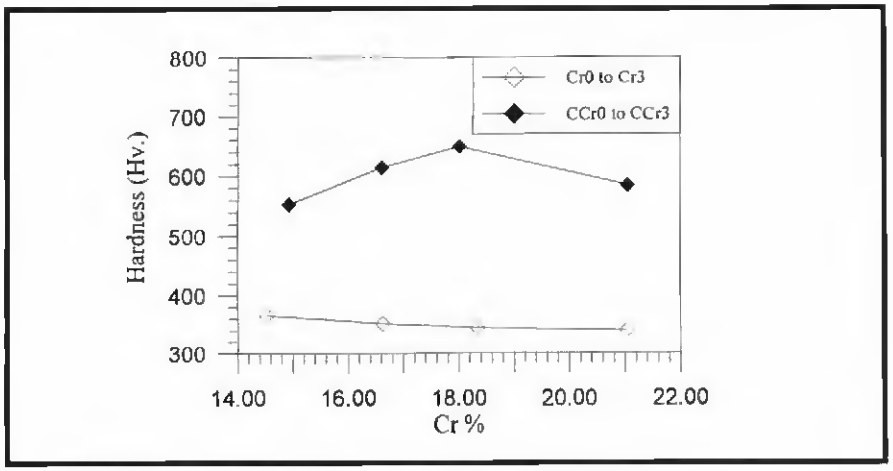

Fig. 8 — The relationship between macrohardness and chromium content.

Table 2—Chemical Composition of AWS Nickel Based Hardfacing Alloys

	C	Cr	Fe	Si	B	Ni
RNiCr-A	0.3–0.6	8–14	1.26–3.25	1.25–3.25	2–3	Rem
RNiCr-B	0.4–0.8	10–16	3–5	3–5	2–4	Rem
RNiCr-C	0.5–1.0	12–18	3.5–5.5	3.5–5.5	2.5–4.5	Rem

Table 3—Abrasive Wear Test Results Showing Weight Loss in Deposit Layers

	Quartz	Silicon Carbide		Quartz	Silicon Carbide
Nb0	0.54	4.73	Cr0	0.52	5.10
Nb1	0.86	4.54	Cr1	0.63	5.02
Nb2	0.62	4.65	Cr2	0.75	5.85
Nb3	0.50	4.80	Cr3	0.81	5.69
CNb0	0.41	5.53	CCr0	0.13	3.11
CNb1	0.33	4.25	CCr1	0.11	2.80
CNb2	0.36	5.16	CCr2	0.10	2.34
CNb3	0.32	3.76	CCr3	0.12	3.68

(unit: gram)

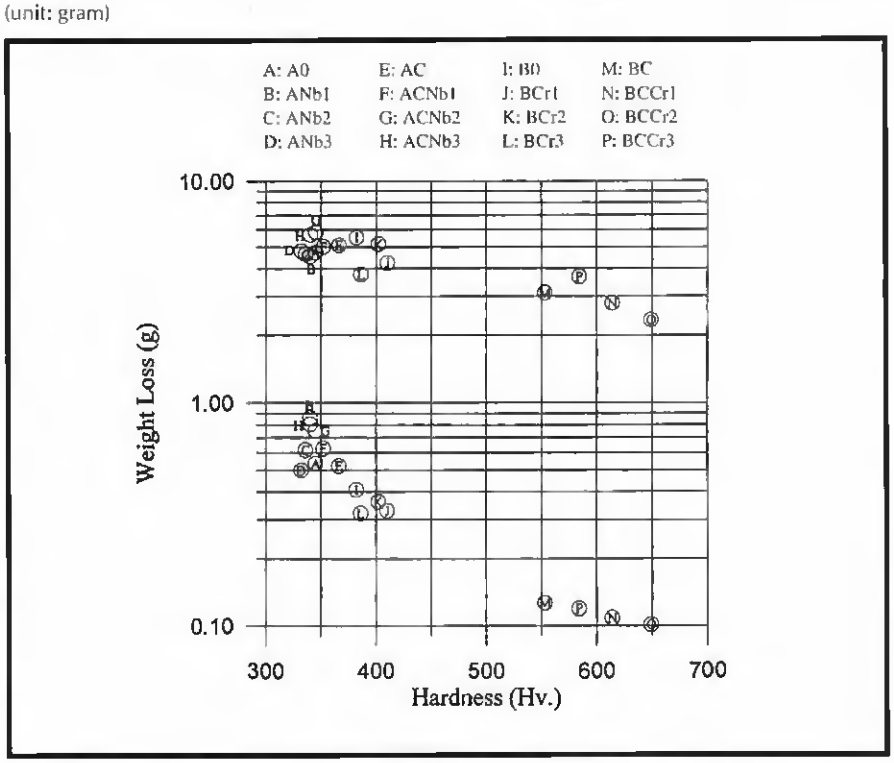

Fig. 9 — The deposit layer weight loss results as determined by the abrasive wear test.

niobium carbide particle is spherical and uniformly distributed throughout the material, so during the processes of wear, when the niobium carbide was pulled out, as shown in Fig. 12, it would roll between the contact faces, reducing the friction coefficient. Figure 13 shows the friction coefficient curves tested on No. Nb1 and No. Nb3, respectively. In both curves, the friction coefficient was found to decrease from about f = 2.3 to about f = 1.7. As for the addition of chromium, the relationship between the macrohardness of deposit layers and wear scar depth was not significant. But when chromium and carbon were added simultaneously, the macrohardness related directly to wear scar depth—the macrohardness increasing as the wear scar depth decreased. According to those results, the macrohardness as well as the microstructure of the materials would affect wear resistance of under dry wear condition.

Figure 14 shows the results of the SRV adhesive wear test using HD150 oil as lubricant. The upper specimen was Cr steel ball (Hv = 746). The result shows that, regardless of the alloy element added to the flux, wear scar depth gradually decreased when macrohardness of the deposit layers increased. With the addition of lubricant between the contact surfaces, the effect on wear resistance from the macrohardness was more important than from the microstructure of the same material.

Corrosion Test

In addition to high hardness and better wear resistance, nickel based hardfacing alloys also have good corrosion resistant properties, so they are usually used in a corrosive environment. With the addition of alloy elements, especially carbon, the wear resistance of the deposit layers improves but the corrosion resistance may be adversely affected. For example: the addition of chromium imparts an improved resistance to oxidizing media, such as nitric acid solution, but not to hydrochloric acid solution. In corrosion resistant alloys, niobium was added as a stabilizing element to bind the carbon and prevent intergranular corrosion attack from grain boundary carbide precipitation. As for carbon, though it creates carbide precipitate and raises the hardness and wear resistance of the deposit layers, the precipitates usually formed on the grain boundary, which could deplete matrix elements. This depletion would lead to intergranular corrosion, and reduce the corrosion

Table 4—Abrasive Wear Test Results Showing Wear Scar Depth in Deposit Layers

	Dry Wear	HD150 Oil		Dry Wear	HD150 Oil
Nb0	63	14.3	Cr0	59	14.0
Nb1	58	14.6	Cr1	56	15.7
Nb2	55	15.4	Cr2	53	16.2
Nb3	54	16.1	Cr3	56	17.2
CNb0	56	11.9	CCr0	46	5.7
CNb1	52	7.8	CCr1	38	3.6
CNb2	51	8.3	CCr2	30	3.2
CNb3	52	10.7	CCr3	38	5.0

(unit: gram)

resistance of the deposit layers (Ref. 17). Figures 15A and B show the weight loss condition of each specimen after having been placed in a concentrated (20%) nitric acid solution and a hydrochloric acid solution for 100 h, respectively. By comparing these figures, we found that, in nickel based hardfacing alloys, the chromium dissolving in the matrix improved resistance to nitric acid corrosion, but adversely affected resistance to corrosion caused by hydrochloric acid. As a result, increasing the chromium content in the deposit layer improved resistance to nitric acid corrosion, but elevated weight loss in hydrochloric acid considerably. When niobium was added it stabilized the carbide, and improved corrosion resistance in the deposit layers. Niobium's ability to combine with carbon instead of chromium resulted in an increase of the chromium content on the matrix. Consequently, the addition of niobium offset the corrosion from the nitric acid. If only

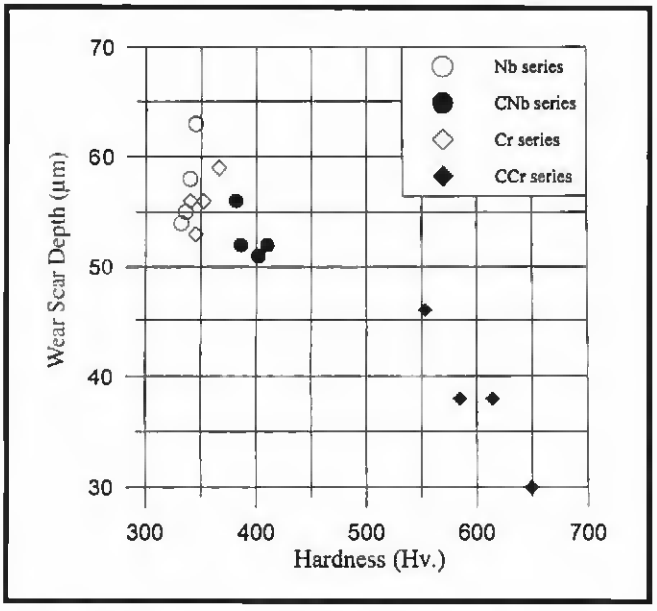

Fig. 10 — The results of the SRV adhesive wear test under dry wear condition.

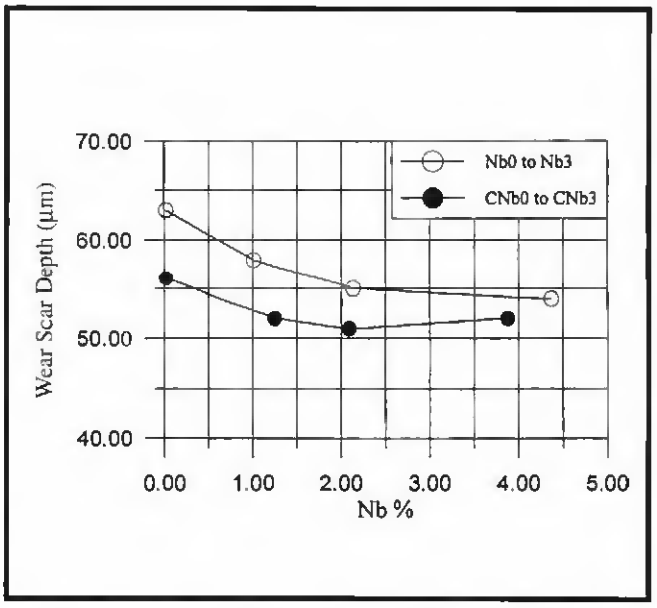

Fig. 11 — The relationship between niobium content and wear scar depth.

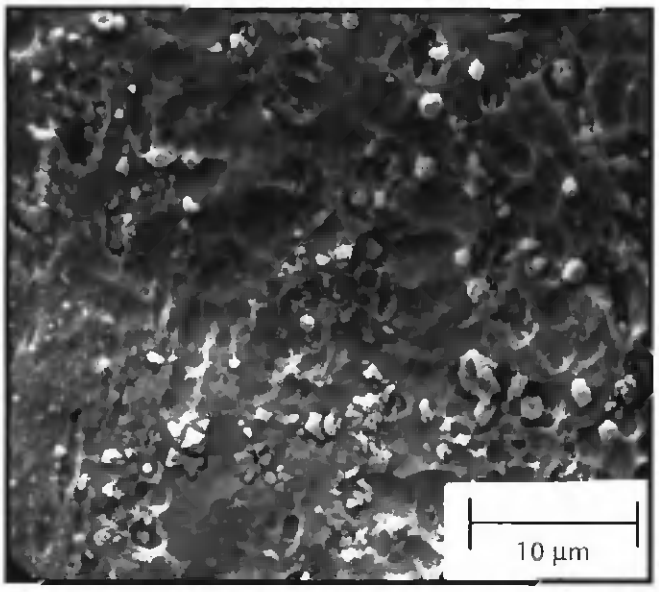

Fig. 12 — Nb-carbide particles appear on the worn surface of Specimen No. Nb3, worn by Si_3N_4 ceramic ball under dry wear condition.

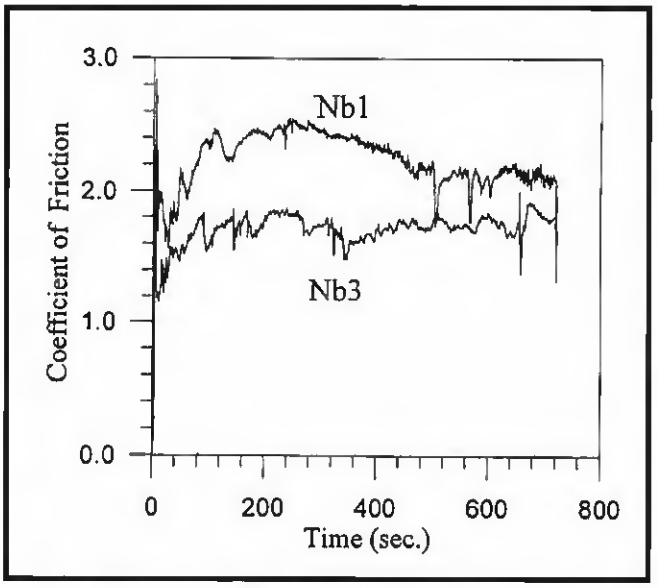

Fig. 13 — The friction curve of the SRV adhesive wear test under dry wear condition.

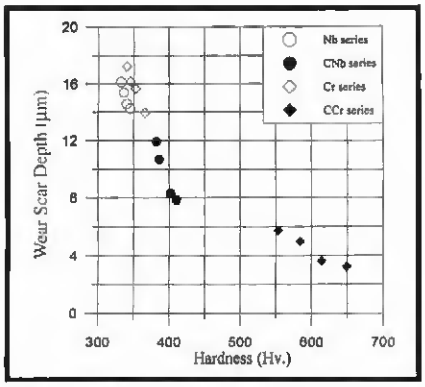

Fig. 14 — SRV adhesive wear test results using HD150 oil as lubricant.

carbon were added to the deposit layer, its weight loss in nitric acid would be elevated considerably, but in hydrochloric acid it would decrease, and as a result, the carbon could deplete the chromium content in the matrix. Adding carbon and niobium to the deposit layers at the same time had slight effects on corrosion resistance, in either nitric acid or hydrochloric acid.

Conclusion

1) Adding niobium to the deposit layers, on one hand, will precipitate spherical niobium carbide particles to reduce the friction coefficient of the wear process, and thus decrease wear loss. On the other hand, if niobium is substituted for chromium, it will increase the latter content in the matrix and raise the corrosion resistance of the deposit layer in nitric acid.

2) No obvious effect on the hardness and wear resistance were found when only chromium was added to the deposit layers, but it may help to improve corrosion resistance in nitric acid. When carbon and chromium were added into the deposit layers simultaneously, the hardness and wear resistance of the deposit layer could be increased, but that was not beneficial to the samples in the nitric acid.

3) Concerning abrasive wear, when the abrasive particles were silicon carbide, because of its high hardness, the increase of the volume fraction of the hard phase had only a slight effect on improving the wear resistance of the deposit layers. But if the abrasive particles were quartz, because of its lower hardness, the increase of the volume fraction of the hard phase could improve the wear resistance of the deposit layers.

4) On adhesive wear, under the dry wear condition, not only the macrohardness but also the microstructure could affect the wear resistance of the deposit layers. However, when HD150 oil was used, the macrohardness of the deposit layers were the main factor determining wear resistance.

5) The corrosion resistance of the nickel based hardfacing alloys was mainly affected by chromium content in the matrix. Increasing the chromium content was advantageous to resist the attack of nitric acid, but it was detrimental to hydrochloric acid resistance.

References

1. Bransal, K. J. Wear of coefficient of hardfacing materials. *Wear Control Handbook*, pp. 373–383.

2. Spencer, D. 1988. Hardfacing processes and practice. *Welding Review*, May, p. 84.

3. Eyre, T. S. 1987. Selecting the optimum surfacing technique for wear resistance. *Second International Conference on Surface Engineering.*

4. Grainger, S. 1986. Repair and reclamation surfacing by welding. *Repair and Reclamation*, Paper 2.

5. Kruschov, M. W. 1974. Principles of abrasive wear. *Wear* 28, pp. 69–88.

6. Rabinowicz, E. 1958. Coefficients predict wear of metal parts. *Product Engineering*, June 23, pp. 71–73.

7. Berns, H., and Fischer, A. 1985. Abrasive wear resistance and microstructure of Fe-Cr-C-B hard surfacing weld deposits. *Wear of Materials*–1985, ASME, pp. 625–633.

8. Silence, W. L. 1987. Effect of structure on wear resistance of Co-, Fe-, and Ni-base. *Wear of Materials*–1987, ASME, pp. 77–85.

9. Bhansali, K. J. 1979. Adhesive wear of nickel- and cobalt-base alloys. *Wear of Materials*–1979, ASME, pp. 146–155.

10. Bhansali, K. J., and Miller, A. E. 1981. Role of stacking fault energy on the galling and wear behavior of a cobalt base alloy. *Wear of Materials*–1981, ASME, pp. 179–185.

11. Sandt, A. 1986. Flame sprayed and fused Ni-Cr-B-Si coatings with additives: characterization and wear behavior. *Surfacing Journal International*, Vol. 1, No. 4, pp. 133–137.

12. Berns, H., Fischer, A., and Theisen, W. 1987. Abrasive wear resistance and microstructure of Ni-Cr-B-Si hardfacing alloys with additions of Al, Nb, Mo, Fe, Mn and carbon. *Wear of Materials*–1987, pp. 535–542.

13. ASTM G65-81. *Standard Practice for Conduction Dry Sand/Rubber Wheel Abrasion Tests.*

14. AWS A5.13. *Specification for Solid Surfacing Welding Rod and Electrodes.*

15. Budinski, K. G. 1988. *Surface Engineering for Wear Resistance.* Chap. 10, pp. 269–271.

16. Hurrick, P. L. 1973. *Some metallurgical factors controlling the adhesive and abrasive wear resistance of steels. Wear* 26. pp. 285–304.

17. ASM. 1983. *Metals Handbook*, Vol. 13, pp. 641–650.

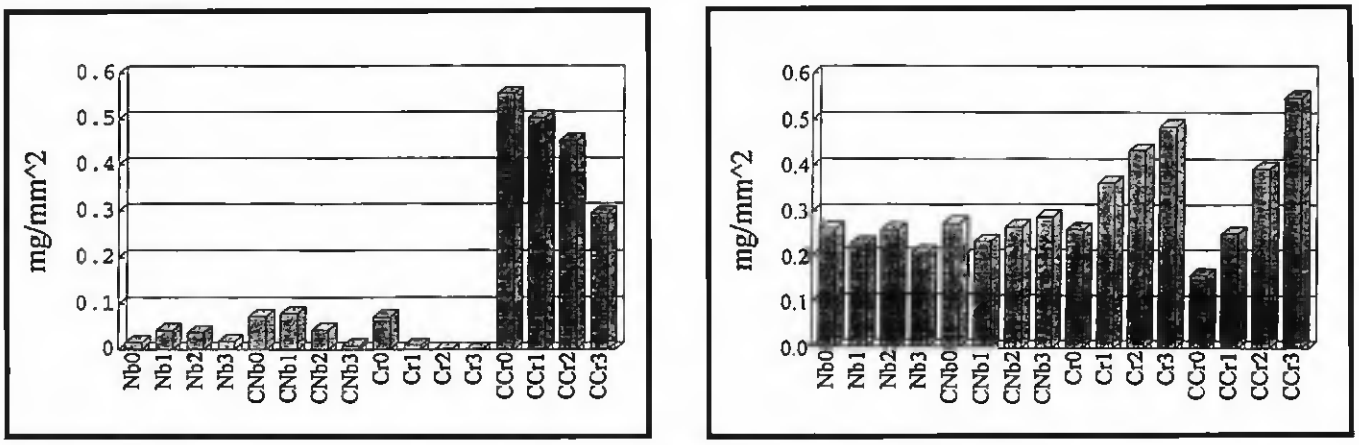

Fig. 15 — The weight loss of the corrosion test. A — 20% HNO3. B — 20% HC1.